



Cytokinin Signaling in *Mycobacterium tuberculosis*

Marie I. Samanovic,^a Hao-Chi Hsu,^b Marcus B. Jones,^{c*} Victoria Jones,^d Michael R. McNeil,^d Samuel H. Becker,^a Ashley T. Jordan,^a Miroslav Strnad,^e Changcheng Xu,^f Mary Jackson,^d Huilin Li,^b K. Heran Darwin^a

^aDepartment of Microbiology, New York University School of Medicine, New York, New York, USA

^bVan Andel Research Institute, Grand Rapids, Michigan, USA

^cHuman Longevity, Inc., San Diego, California, USA

^dMycobacteria Research Laboratories, Department of Microbiology, Immunology and Pathology, Colorado State University, Fort Collins, Colorado, USA

^eLaboratory of Growth Regulators, Centre of the Region Haná for Biotechnological and Agricultural Research, Institute of Experimental Botany ASCR and Palacký University, Olomouc, Czech Republic

^fBiology Department, Brookhaven National Laboratory, Upton, New York, USA

ABSTRACT It was recently reported that the human-exclusive pathogen *Mycobacterium tuberculosis* secretes cytokinins, which had only been known as plant hormones. While cytokinins are well-established, adenine-based signaling molecules in plants, they have never been shown to participate in signal transduction in other kingdoms of life. *M. tuberculosis* is not known to interact with plants. Therefore, we tested the hypothesis that cytokinins trigger transcriptional changes within this bacterial species. Here, we show cytokinins induced the strong expression of the *M. tuberculosis* gene Rv0077c. We found that Rv0077c expression is repressed by a TetR-like transcriptional repressor, Rv0078. Strikingly, cytokinin-induced expression of Rv0077c resulted in a loss of acid-fast staining of *M. tuberculosis*. While acid-fast staining is thought to be associated with changes in the bacterial cell envelope and virulence, Rv0077c-induced loss of acid-fastness did not affect antibiotic susceptibility or attenuate bacterial growth in mice, consistent with an unaltered mycolic acid profile of Rv0077c-expressing cells. Collectively, these findings show cytokinins signal transcriptional changes that can affect *M. tuberculosis* acid-fastness and that cytokinin signaling is no longer limited to the kingdom Plantae.

IMPORTANCE Cytokinins have only previously been known as plant hormones. The discovery that they can be used as signaling molecules outside of plants broadens the repertoire of small molecules that can potentially affect gene expression in all domains of life.

KEYWORDS *Mycobacterium tuberculosis*, acid-fast staining, cytokinin, regulation, signaling

Mycobacterium tuberculosis is the causative agent of tuberculosis, one of the world's leading causes of mortality (1). For this reason, researchers are eager to identify pathways that could be targeted for the development of new therapeutics to treat this devastating disease. Among the current prioritized targets is the mycobacterial proteasome. *M. tuberculosis* strains with defects in proteasome-dependent degradation are highly attenuated in mice, partly because they are sensitive to nitric oxide (NO) (2–7). The NO-sensitive phenotype of mutants defective for proteasomal degradation has been attributed to a failure to degrade an enzyme called Log (Lonely guy), a homologue of a plant enzyme involved in the synthesis of a family of *N*⁶-substituted adenine-based molecules called cytokinins (CKs) (8). The accumulation of Log in *M. tuberculosis* results in a buildup of cytokinins, which can break down into aldehydes that effectively sensitize mycobacteria to NO (8).

Received 3 May 2018 Accepted 17 May 2018 Published 19 June 2018

Citation Samanovic MI, Hsu H-C, Jones MB, Jones V, McNeil MR, Becker SH, Jordan AT, Strnad M, Xu C, Jackson M, Li H, Darwin KH. 2018. Cytokinin signaling in *Mycobacterium tuberculosis*. *mBio* 9:e00989-18. <https://doi.org/10.1128/mBio.00989-18>.

Invited Editor David R. Sherman, Seattle Biomedical Research Institute

Editor E. Peter Greenberg, University of Washington

Copyright © 2018 Samanovic et al. This is an open-access article distributed under the terms of the [Creative Commons Attribution 4.0 International license](https://creativecommons.org/licenses/by/4.0/).

Address correspondence to Huilin Li, Huilin.Li@vai.org, or K. Heran Darwin, heran.darwin@med.nyu.edu.

* Present address: Marcus B. Jones, Regeneron Pharmaceuticals, Inc., Tarrytown, New York, USA.

M.I.S. and H.C.H. contributed equally to this article.

TABLE 1 Bacterial strains and plasmids used in this study

Strain or plasmid	Relevant genotype	Source or reference
Strains		
<i>M. tuberculosis</i>		
H37Rv	Wild type (WT)	ATCC 25618
MHD18	Hyg ^r WT with pMV306	3
MHD761	Strep ^r WT with pMV306.strep	8
MHD794	Kan ^r WT with pMV306.kan	44
MHD1033	Kan ^r Rv0077c::MycMarT7 with transposon insertion between codons 64 and 65	This work
MHD1077	Kan ^r Strep ^r MHD1033 with pMV306.strep-Rv0077c	This work
MHD1086	Kan ^r Strep ^r MHD1033 with pMV306.strep	This work
MHD1293	Hyg ^r ΔRv0078::hyg	This work
MHD1315	Hyg ^r Kan ^r ΔRv0078::hyg with pMV306.kan	This work
MHD1316	Hyg ^r Kan ^r ΔRv0078::hyg with pMV306.kan-Rv0078 _{W100R}	This work
MHD1318	Hyg ^r Kan ^r ΔRv0078::hyg with pMV306.kan-Rv0078	This work
<i>E. coli</i>		
ER2566	F ⁻ λ ⁻ <i>fhuA2</i> [lon] <i>ompT lacZ::T7 genel gal sulA11</i> Δ(<i>mcrC-mrr</i>)114::IS10R(<i>mcr-73</i> ::miniTn10) 2R(<i>zgb-210</i> ::Tn10)1 (Tet ^s) <i>endA1</i> [dcm]	45
DH5α	F ⁻ φ80dlacZΔM15 Δ(<i>lacZYA-argF</i>)U169 <i>deoR recA1 endA1 hsdR17</i> (r _k ⁻ m _k ⁺) <i>phoA supE44</i> λ <i>thi-1 gyrA96 relA1</i>	Gibco, BRL
Plasmids		
pET24b(+)	Kan ^r plasmid for production of C-terminal His ₆ epitope-tagged protein	Novagen
pMV306.kan	Kan ^r plasmid that integrates at <i>attB</i> site on <i>M. tuberculosis</i> chromosome	46
pMV306	Hyg ^r plasmid that integrates at <i>attB</i> site on <i>M. tuberculosis</i> chromosome	46
pMV306.strep	Strep ^r plasmid that integrates at <i>attB</i> site on <i>M. tuberculosis</i> chromosome	Gift from John McKinney
pYUB854	Hyg ^r allelic exchange vector	34
pMV306.strep-Rv0077c	Strep ^r pMV306.strep plasmid with Rv0077c and 200 bp upstream of start codon of Rv0077c	This work
pMV306.kan-Rv0078	Kan ^r pMV306.kan plasmid with Rv0078 and 200 bp upstream of start codon of Rv0078	This work
pMV306.kan-Rv0078 _{W100R}	Kan ^r pMV306.kan-Rv0078 plasmid with Trp100 changed to Arg	This work
pET24b(+)-Rv0077cHis ₆	Kan ^r ; for production of Rv0077c-His ₆ in <i>E. coli</i>	This work
pET24b(+)-Rv0078His ₆	Kan ^r plasmid for production of Rv0078-His ₆ in <i>E. coli</i>	This work

While we determined that a lack of proteasome-dependent degradation results in cytokinin accumulation, we were left with more questions, namely, what is the function of cytokinin production by *M. tuberculosis*? In plants, cytokinins are hormones that regulate growth and development (9). In addition, bacterial plant pathogens and symbionts use cytokinins to facilitate the parasitism of their plant hosts (10). Outside of the laboratory, *M. tuberculosis* exclusively infects humans and is not known to have an environmental reservoir; therefore, it is unlikely *M. tuberculosis* secretes cytokinins to modulate plant development. Instead, we hypothesized that *M. tuberculosis*, like plants, uses cytokinins to signal intraspecies transcriptional changes to its benefit. Here, we show that cytokinins induce the transcription of a gene of unknown function. Moreover, we identified and characterized a TetR-like regulator that represses the expression of this gene. While we have not yet identified an *in vivo* phenotype associated with this cytokinin-inducible gene, we found that its expression altered the cell envelope of *M. tuberculosis*, changing its staining properties. Collectively, these studies provide a foundation to characterize cytokinin signaling in *M. tuberculosis* and other cytokinin-producing bacterial species.

RESULTS

Cytokinins induce the specific and high expression of Rv0077c in *M. tuberculosis*. To test if a cytokinin (CK) could induce gene expression in *M. tuberculosis*, we grew wild-type (WT) *M. tuberculosis* H37Rv to mid-logarithmic phase and incubated the bacteria for 5 h with *N*⁶-(Δ²-isopentenyl)adenine (iP), one of the most abundantly produced cytokinins in *M. tuberculosis*, which is also commercially available (8) (see Materials and Methods and Tables 1 and 2 for strains, plasmids, primers, and probes). Using high-throughput RNA sequencing (RNA-Seq), we discovered the expression of four genes, Rv0076c, Rv0077c, Rv0078, and *mmpL6*, was significantly induced upon iP treatment compared to treatment with the vehicle control (dimethyl sulfoxide [DMSO])

TABLE 2 Sequences of the primers and probes used in this study

Primer or probe	Sequence ^a	Purpose
Primers		
F2Rv0077cNde1	CAGTCAT ATG TCGACGATCGACATTAGTGCCG	For cloning into pET24b(+)
R20077cHindIII	GTCT AAGCTT CGTGCACCGCGACCGTCGACAACTG	For cloning into pET24b(+)
F2Rv0078Nde1	TAGTCATATGAAATCAAGAGACGCACCCAGGAG	For cloning into pET24b(+)
R20078HindIII	AATG AAGCTT GCCGTTAAGCATCCCGTCGATGAG	For cloning into pET24b(+)
F3Rv00777cFISH	TGACCCCGCCTCGGTGCGGATTTCGG	For mutant mining of Rv0077c::MycMarT7
F5Rv0077cNhe1	TATCGCTAGCTGACCCCGCCTCGGTGCGGATTTCGG	Rv0077c complementation in <i>M. tuberculosis</i> in pMV306.strep
R4Rv0077cHindIII	AGGTAAGCTTCTACGTGCGCACCGCGACCGTCGACAACTG	Rv0076c-Rv0077c complementation in <i>M. tuberculosis</i> in pMV306.strep
R4Rv0076cHindIII	TAGTAAGCTTTCACAACGCTGCGGCGTGTGGGTC	Rv0076c-Rv0077c complementation in <i>M. tuberculosis</i> in pMV306.strep
R2Rv00785Race	CCAGGCATCGACCGCTGCCCCG	5' RACE of Rv0078
R2Rv0077c5Race	GCCGGTGTGTTGCCGACAGCA	5' RACE of Rv0077c
R1Rv0077c5Race	GCGACGAGCTGGGTGACGAC	5' RACE of Rv0077c
R1Rv00785Race	GGATCACCAGATACCTCGAG	5' RACE of Rv0078
F5Rv0078Nhe1	TATCGCTAGCGACCGGCGAGTGCCTACTGACCCGTCGCCATAG	Rv0078 complementation in pMV306.kan
R5Rv0078HindIII	CGGTAAGCTTCTAGCCGTTAAGCATCCCGTCGATG	Rv0078 complementation in pMV306.kan
EMSA probes		
+74/+32	AATGAATAGTTCGGGACTAATGTCGATCGTCGACATGGATGCCAGACCAGGGGCAC	
+8/-25	AGCAGACTGCCGGTAACTTACCAACAGATTGTACCAGACCAGGGGCAC	
+19/-14 (WT)	GTACATTTACAAGCAGACTGCCGGTAACTTACCCAGACCAGGGGCAC	
+19/-14 NS11	GTACATGATAAAGCAGACTGCCTAGTGATAGTGCCAGACCAGGGGCAC	
+19/-14 NS21	GTACATGATAGTAGTAGTGATGATGATCTTACCCAGACCAGGGGCAC	
+19/-14 NS27	GTACATGATAGTAGTAGTGATGATGATATAGTGCCAGACCAGGGGCAC	
14merScaffold5IRDye700	5'-5IRD700-GTGCCCTGGTCTGG	

^aIn the primer sequences, changes to the normal sequence are in boldface. In the probe sequences, the 14-nucleotide oligomers are underlined.

(Fig. 1A; see Table S1 in the supplemental material). Rv0077c is conserved among many mycobacterial species, while Rv0076c and Rv0078 are present only in several mycobacterial genomes (Fig. 1B) (11). Notably, *Mycobacterium smegmatis*, a distant, non-pathogenic relative of *M. tuberculosis*, has a weak homologue of Rv0077c and no conspicuous Rv0078 homologue (Fig. 1B). *mmpL6* is one of 13 *mmpL* (*mycobacterial membrane protein large*) genes in *M. tuberculosis*. In strain H37Rv, *mmpL6* is predicted to encode a 42-kDa protein with five transmembrane domains and is truncated compared to the same gene in ancestral tuberculosis strains (12). Thus, it is unclear if *mmpL6* encodes a functional protein in strain H37Rv.

Rv0077c was by far the most strongly induced gene in *M. tuberculosis* upon iP treatment; therefore, we chose it for follow-up studies. We raised polyclonal antibodies to recombinant Rv0077c protein and showed that protein levels were increased in *M. tuberculosis* treated with iP for 24 h (Fig. 1C, first two lanes). Rv0077c was barely detectable in cell lysates of bacteria that had not been incubated with iP and was undetectable in a strain with a transposon insertion mutation in Rv0077c (Fig. 1C, center two lanes). Rv0077c protein was restored to WT levels in the mutant upon complementation with an integrative plasmid carrying Rv0077c expressed from its native promoter (Fig. 1C, last two lanes). We also found a dose-dependent induction of Rv0077c production using iP concentrations from 1 nM to 100 μ M (Fig. 1D).

We next synthesized and tested if the most abundantly produced cytokinin in *M. tuberculosis*, 2-methylthio-iP (2MeSiP) (8), could also induce Rv0077c production. 2MeSiP strongly induced Rv0077c production (Fig. 1E, lane 4). Importantly, we did not observe induction of Rv0077c when we incubated the bacteria with the appropriate cytokinin riboside (R) precursors iPR or 2MeSiPR (Fig. 1E, lanes 3 and 5). Similarly, AMP or the closely related molecule adenine could not induce Rv0077c expression (Fig. 1E, lanes 6 and 7). We hypothesized while adenine could not induce Rv0077c expression, at high enough concentrations, it could possibly inhibit Rv0077c induction by com-

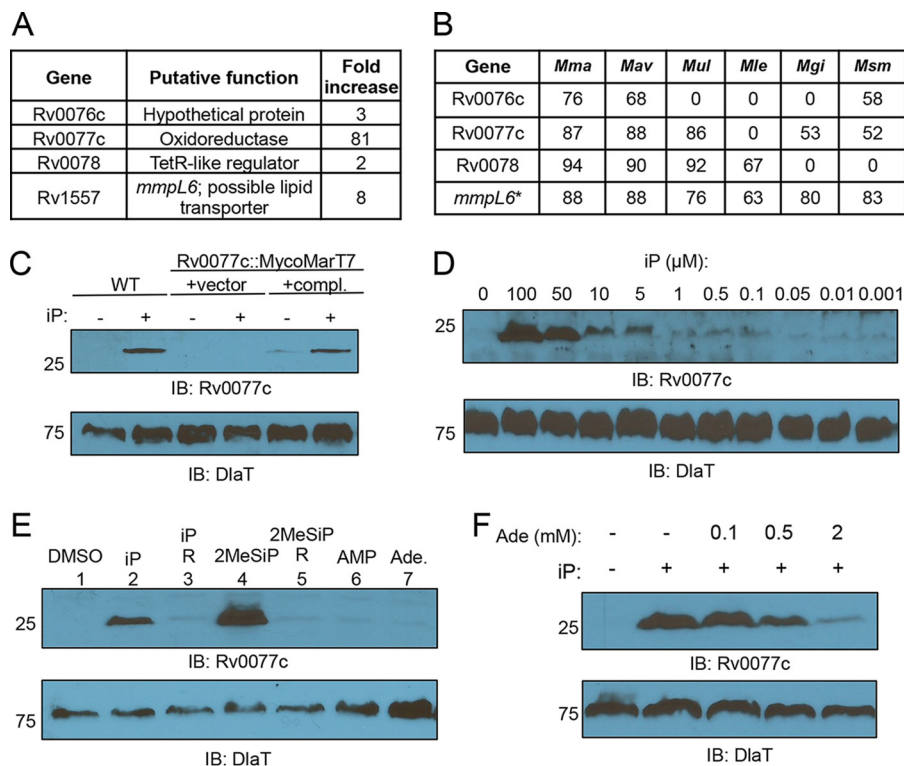


FIG 1 Cytokinins induce the expression of Rv0077c in *M. tuberculosis*. (A) Genes significantly regulated by the presence of 100 μ M iP for 5 h as analyzed by RNA-Seq. (B) Percentage of identity between *M. tuberculosis* H37Rv proteins and proteins of targeted mycobacterial genomes, including *M. marinum* (Mma), *M. avium* (Mav), *M. ulcerans* (Mul), *M. leprae* (Mle), *M. gilvum* (Mgi), and *M. smegmatis* (Msm). An asterisk indicates *mmpL6* encodes a truncated protein in H37Rv, unlike in the other mycobacterial species in the table. (C) Immunoblot for Rv0077c in total cell lysates of WT *M. tuberculosis*. "compl." indicates complemented. iP was used at a final concentration of 100 μ M when added. (D) Dose-dependent production of Rv0077c protein. Bacteria were incubated with cytokinin at the indicated concentrations for 24 h. (E) Only cytokinins, and not closely related molecules, induce the production of Rv0077c. Each compound was added to a final concentration of 100 μ M. "R" indicates the riboside form of the preceding indicated cytokinin. (F) Adenine inhibits the induction of Rv0077c by 100 μ M iP. For all panels, we added an equal volume of DMSO to samples where iP was not added. For all immunoblots (IB), we stripped the membranes and incubated them with antibodies to dihydrolipoamide acyltransferase (DiaT) to confirm equal loading of total lysates. Molecular weight standards are indicated to the left of the blots and are in kilodaltons (kDa). Ade, adenine.

peting with cytokinin for access to a transporter or receptor. Indeed, adenine reduced the induction of Rv0077c by iP in a dose-dependent manner (Fig. 1F).

Identification of an operator for the TetR-like transcriptional repressor Rv0078.

Rv0077c is divergently expressed from Rv0078; the proposed translational start codons for these genes are separated by 61 bp. Based on its cytokinin-dependent expression and its proximity to Rv0077c, we hypothesized that Rv0078 encodes a repressor of both genes. We identified the promoter regions for each gene by performing rapid amplification of 5' cDNA ends (5' RACE) analysis of Rv0077c and Rv0078 and determined the likely start of transcription for one gene was within the 5' untranslated region of the other gene (Fig. 2A). We sought to identify an operator sequence by using an electrophoretic mobility shift assay (EMSA) (Fig. 2B). We narrowed down a putative Rv0078 binding site to a region overlapping the proposed starts of transcription (+1) of both Rv0077c and Rv0078 (Fig. 2A, red box). TetR-like regulators generally bind to inverted repeat sequences; we identified a 21-bp sequence within positions $-14/+19$ (relative to position +1) of Rv0077c containing two 10-bp inverted repeat sequences. Mutagenesis of the probe in the repeat sequences disrupted Rv0078 binding to the DNA (Fig. 2B). Importantly, the binding sequence overlaps the putative transcriptional start sites of both genes, suggesting that expression of both genes is repressed by Rv0078.

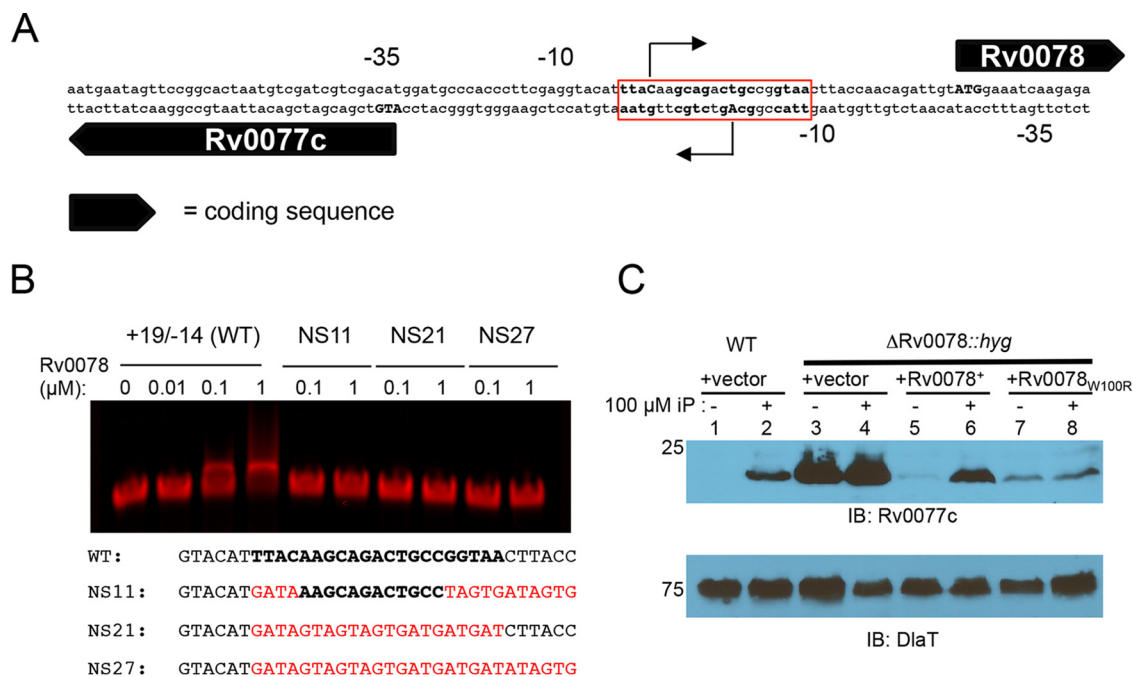


FIG 2 Rv0078 represses the expression of Rv0077c. (A) The putative transcriptional start sites (+1) of Rv0077c and Rv0078 as determined by 5' RACE and represented as bent arrows. The predicted start codons are in capital boldface letters. (B) EMSA analysis identifies a putative repressor binding site. Probe sequence +19/−14 refers to positions relative to Rv0077c position +1. In boldface is the presumed binding site. Mutated residues are in red. Not shown at the end of each probe is a sequence for annealing to a fluorescent tag (Table S1). Rv0078 was purified under native conditions from *E. coli*. (C) Deletion and disruption of Rv0078 result in the constitutive expression of Rv0077c. Total cell lysates were prepared and separated on a 10% SDS-PAGE gel. IB, immunoblot. The membrane was stripped and then incubated with antibodies to DlaT to confirm equal loading of samples. Molecular weight standards are indicated to the left of the blots and are in kilodaltons (kDa).

Notably, the addition of iP did not result in the release of Rv0078 from the DNA probe (Fig. 2B; see Fig. S1 in the supplemental material). Therefore, cytokinins do not appear to directly bind to Rv0078 to induce gene expression.

Based on the 5' RACE analysis, we were able to delete and replace most of the Rv0078 gene with the hygromycin resistance gene (*hyg*) without disrupting the promoter of Rv0077c in *M. tuberculosis* H37Rv. A Δ Rv0078::hyg strain displayed constitutively high expression of Rv0077c irrespective of the presence of cytokinin, supporting a model in which Rv0078 directly represses Rv0077c expression (Fig. 2C). A single copy of Rv0078 expressed from its native promoter restored iP-regulated control of Rv0077c in this strain (Fig. 2C, lanes 5 and 6). Interestingly, in the process of making the complementation plasmid, we acquired a random mutation (likely generated during PCR) in Rv0078 that changed a tryptophan to arginine (W100R); this allele was unable to restore cytokinin-dependent regulation of Rv0077c to the Δ Rv0078::hyg strain (Fig. 2C, lanes 7 and 8).

Two Rv0078 dimers bind to one operator. To gain an understanding of how Rv0078 represses gene expression, we solved the crystal structure of Rv0078 to 1.85 Å by a single-wavelength anomalous dispersion method. As previously reported, Rv0078 forms dimers resembling other TetR-like proteins (13, 14). Unlike the canonical TetR binding site, *tetO*, which is 15 bp long, the Rv0078 binding site is 21 bp long, suggesting Rv0078 binds to DNA differently than TetR. We performed an isothermal titration calorimetry (ITC) experiment and determined that the apparent K_D (dissociation constant) of Rv0078 for operator DNA was 357 nM (Fig. 3A). The estimated stoichiometry of DNA duplex to Rv0078 dimer was 0.66, suggesting that two Rv0078 dimers bind to one operator sequence.

We next cocrystallized Rv0078 with a 23-bp DNA fragment that was extended 1 bp at each end of the 21-bp operator sequence identified in Fig. 2 (positions −8/+13

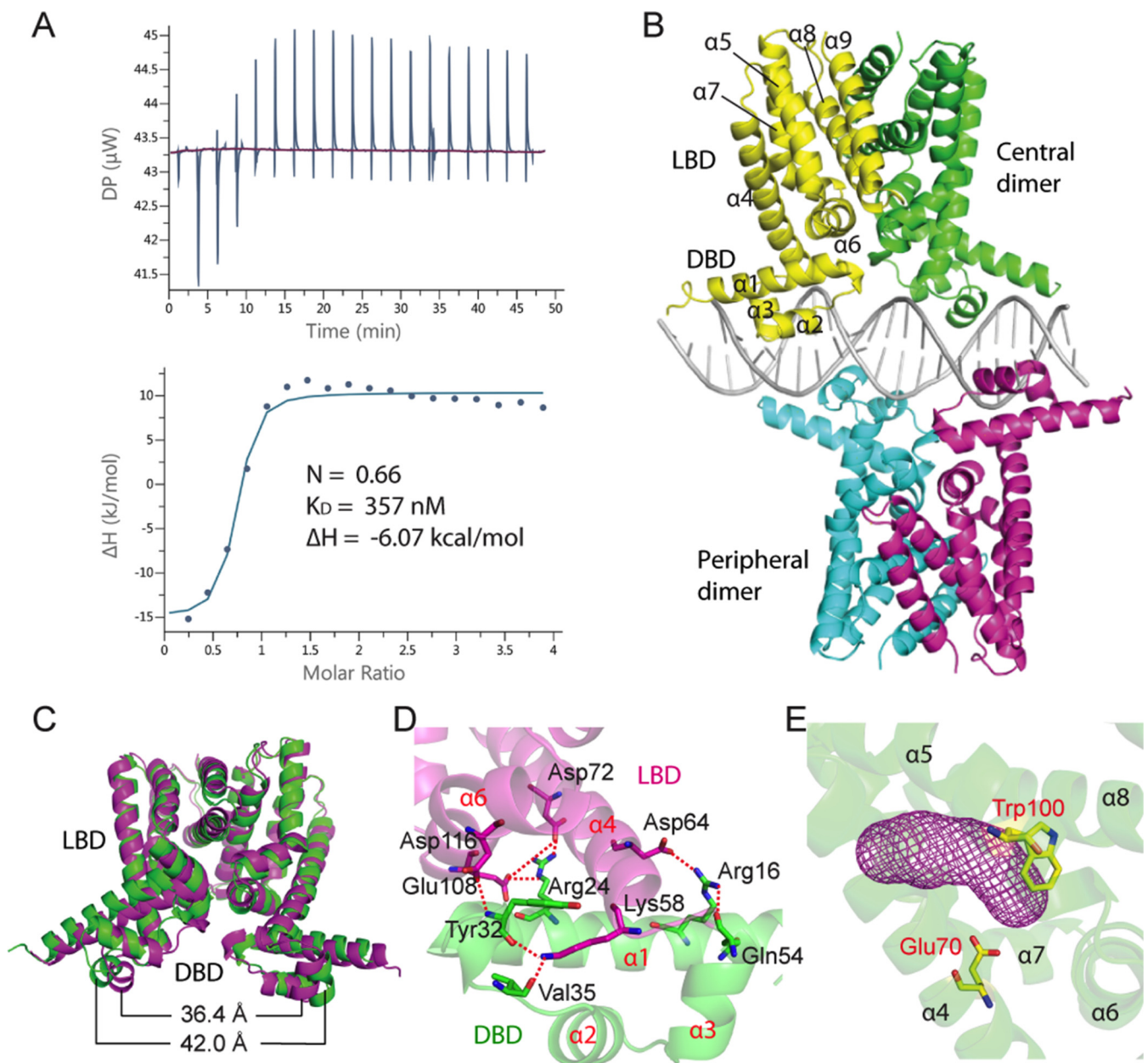


FIG 3 Crystal structure of Rv0078 in complex with DNA. (A) ITC of Rv0078 binding to the +13/−8 DNA probe. The binding stoichiometry, ΔH , and K_D are marked. (B) Overall structure of Rv0078-DNA complex in cartoon view. Two Rv0078 dimers (“central” and “peripheral”) bind to one DNA molecule. (C) The distance between two DNA-binding domains decreases by ~ 6 Å when bound to DNA. The DNA-free Rv0078 is in green, and the DNA-bound Rv0078 is in magenta. (D) Interactions between the LBD (magenta) and DBD (green) in a monomer. (E) The ligand binding pocket (magenta mesh) of Rv0078 is enclosed by a four-helix bundle (helices $\alpha 5$ to $\alpha 8$).

[relative to +1] of Rv0077c) and solved the structure to a resolution of 3.0 Å (Table 3). As predicted by the ITC experiments, we observed two Rv0078 dimers bound to a DNA duplex where each dimer bound on opposite sides of the DNA (Fig. 3B). The top or “central” dimer bound the DNA palindrome symmetrically, while the bottom or “peripheral” dimer bound to DNA off-center, staggered from the central dimer binding site by 7 bp. Thus, the longer-than-canonical (i.e., *tetO*) binding site is required for accommodation of two Rv0078 dimers, unlike TetR, which binds to *tetO* as a single dimer.

Rv0078 has an N-terminal DNA-binding domain (DBD) and a C-terminal ligand-binding domain (LBD) (Fig. 3B to D). DNA binding induced significant conformational changes across the Rv0078 dimer structure, with a root mean square deviation (RMSD)

TABLE 3 Data collection and refinement statistics for Rv0078 with and without DNA

Parameter	Value(s) for ^a :		
	Rv0078	Rv0078 DNA	SeMet Rv0078
Data collection statistics			
Wavelength	0.97931	1.12713	0.97931
Space group	C121	P12 ₁ 1	C121
Unit cell dimensions			
<i>a</i> , <i>b</i> , <i>c</i> (Å)	224.91, 67.07, 56.02	82.04, 82.04, 186.66	219.26, 68.04, 57.49
α , β , γ (°)	90, 99.19, 90	90, 90.07, 90	90, 97.06, 90
Resolution (Å)	111.01–1.85 (1.95–1.85)	28.75–3.0 (3.16–3.00)	108.8–2.7 (2.85–2.7)
<i>R</i> _{merge} (%)	5.1 (42.1)	20.4 (105)	12.6 (47.3)
<i>I</i> / σ	16.97 (2.7)	5.5 (1.8)	12.7 (4.6)
Total reflections	252,128	296,694	175,154
Completeness (%)	96.5 (95.1)	94.8 (100)	99.5 (100)
Redundancy	3.7 (3.5)	6.4 (5.8)	3.9 (3.9)
Refinement statistics			
Resolution (Å)	36.38–1.85	28.5–3.0	
No. of reflections	67,720	46,083	
<i>R</i> _{work} / <i>R</i> _{free} (%)	0.2174/0.2469	0.2019/0.2469	
No. of:			
Nonhydrogen atoms	6,037	13,639	
Macromolecules	5,937	13,639	
Ligand	ND	ND	
Water	100		
<i>B</i> -factors (Å ²)	30.68	69.15	
Macromolecules	30.78	69.15	
Water	24.65		
RMSDs			
Bond lengths (Å)	0.007	0.10	
Bond angles (°)	0.83	1.21	
Ramachandran statistics (%)			
Favored	99.35	97.53	
Allowed	0.65	2.47	
Outliers	0	0	

^aValues in parentheses are for the highest-resolution shell. ND, not determined.

of 2.13 Å compared to the DNA-free dimer. In particular, the two α 3 helices move toward each other by ~6 Å, in order to reduce their distance to 36.4 Å and fit in the DNA major grooves (Fig. 3C). In the LBD, the ligand entry between helices α 4 and α 5 is open and the ligand-binding pocket is empty. It appears that changes initiated in the DBD regions upon binding to the DNA are transmitted to the LBD via the DBD-LBD interface, which involves extensive interactions, including two salt bridges and six H-bonds (Fig. 3D).

The ligand-binding pocket of Rv0078 is largely hydrophobic. Within this pocket, we observed an elongated density resembling a long aliphatic chain of a fatty acid (see Fig. S2 in the supplemental material). Gas chromatography-mass spectrometry (GC-MS) of the compounds extracted from Rv0078 purified from *Escherichia coli* revealed fatty acids commonly found in this organism, and a palmitate molecule fit well with the electron density (Fig. S2A to E). A fatty acid carboxylate formed a hydrogen bond with Rv0078 Glu-70 (Fig. 3E and Fig. S2C), and the long alkyl chain had numerous hydrophobic interactions within the extended ligand pocket. When we purified Rv0078 under denaturing conditions and refolded the protein to remove the lipid, we observed the same EMSA results as we observed with protein purified under native conditions (data not shown), suggesting this fatty acid is unlikely to be the native Rv0078 ligand; however, these data may suggest that the native ligand is fatty acid-like. Interestingly, we found that Trp100 faces the ligand-binding pocket (Fig. 3E), which suggests Trp100 interacts with the natural ligand. This hypothesis is supported by our data showing an Rv0078_{W100R} mutant was unable to complement the Rv0078 deletion mutant strain (Fig. 2C, lane 8).

In addition to characterizing the LBD, we identified 9 amino acids that were important for interacting with DNA (Fig. 4A to E). Specifically, the hydroxyl groups of

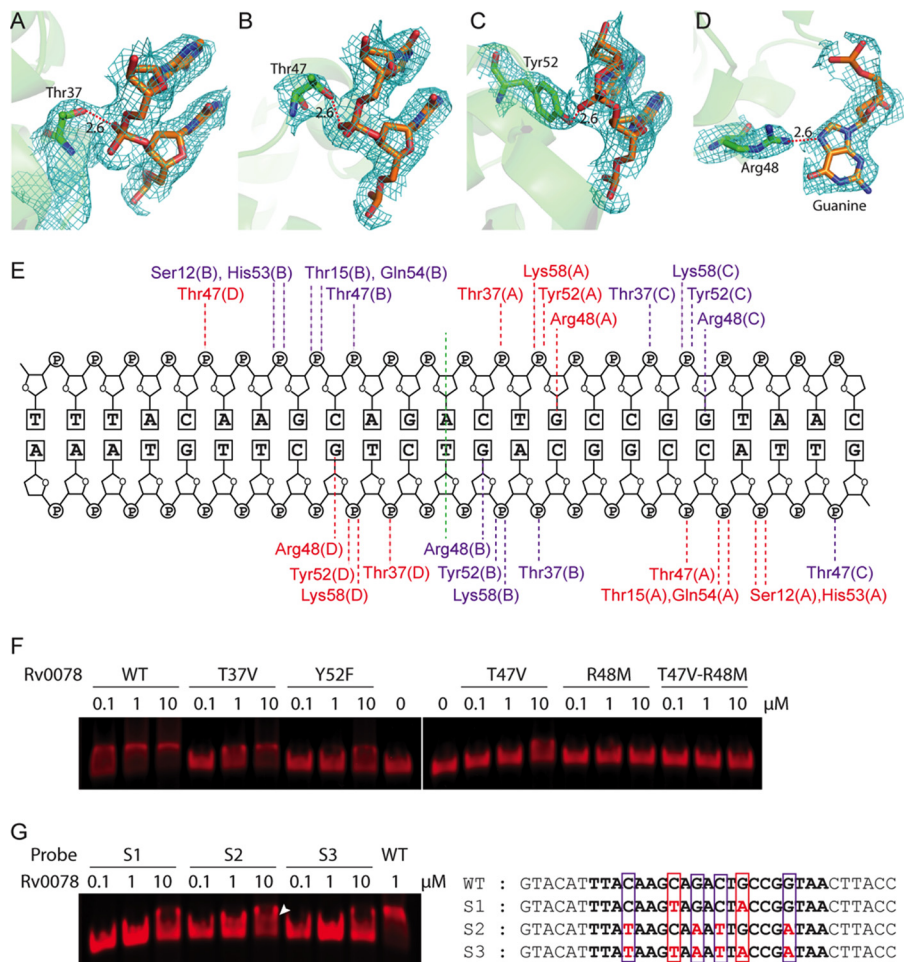


FIG 4 Rv0078-DNA interactions determined by X-ray crystallography. The hydroxyl groups of Thr37 (A), Thr47 (B), and Tyr52 (C) interact with the backbone phosphate with a distance of 2.6 Å. (D) Arg48 interacts with guanine with a distance of 2.6 Å. The $2F_o - F_c$ maps are contoured at the 1σ level. (E) A schematic representation of Rv0078-DNA contacts. Residues of the central dimer are labeled in red, and residues of the peripheral dimer are in purple. (F) EMSA using WT DNA probe and Rv0078 with mutations in Thr37, Thr47, Arg48, or Tyr52. (G, left panel) EMSA of Rv0078 with DNA probes with G-to-A substitutions in the central dimer binding region (S1), peripheral dimer binding region (S2), or in both DNA regions (S3). The white arrowhead marks the partial shift with the S2 probe at high protein concentration. (G, right panel) Sequences of the four DNA probes used in EMSAs. The nucleotides contacting the central dimer are boxed in red, and those contacting the peripheral dimer are boxed in purple.

Thr37, Thr47, and Tyr52 interacted strongly with DNA phosphates at a distance of 2.6 Å. Arg48 is the only residue that interacted with DNA by recognizing a guanine base at a distance of 2.6 Å. To further examine the importance of these residues, we introduced single amino acid substitutions (T37V, T47V, R48M, and Y52F) or double mutations (T47V and R48M) into Rv0078 and performed EMSAs. While all of the mutant proteins were soluble and behaved like the WT protein in solution, Rv0078_{R48M} did not bind to DNA, and the other mutant proteins bound to DNA with reduced affinities (Fig. 4F).

To examine the DNA sequence specificity of Rv0078, we synthesized three EMSA probes by changing the Rv0078 Arg48-interacting guanines to adenines (G-to-A) in the central dimer binding region (probe S1), the peripheral dimer-binding region (probe S2), or both dimer-binding regions (probe S3). These G-to-A substitutions either abolished or compromised Rv0078 binding to DNA, affirming the critical role of guanines in the binding site (Fig. 4G). Notably, substitutions in probe S1 entirely abolished Rv0078 binding, while substitutions in S2 retained a partial gel shift at a high concentration (white arrowhead in Fig. 4G). This observation suggests that the binding of the two Rv0078 dimers is cooperative, with the central dimer likely the first one to bind to DNA.

TABLE 4 Antibiotic IC₅₀s of the WT and Rv0078 strains

Drug	IC ₅₀ for:	
	Parental strain	ΔRv0078::hyg mutant
Ethionamide	1.0–2.3 μg/ml	0.8–1.3 μg/ml
Ciprofloxacin	0.1–0.2 μg/ml	0.1–0.2 μg/ml
Ethambutol	0.6–2 μg/ml	0.6–2 μg/ml
Isoniazid	32–44 ng/ml	29–44 ng/ml
Meropenem ^a	1 μg/ml	1 μg/ml
Norfloxacin	2 μg/ml	2 μg/ml
Rifampin	32–38 ng/ml	32–38 ng/ml
Streptomycin	0.3–0.6 μg/ml	0.3–0.4 μg/ml
Vancomycin ^a	3–10 μg/ml	6–10 μg/ml

^aSupplemented with 5 μg/ml potassium clavalunite. See Materials and Methods for details.

Constitutive expression of Rv0077c does not affect antibiotic susceptibility or virulence in mice. During our ongoing studies, a report was published on the identification of a small molecule of the spiroisoxazoline family, SMART-420, which strongly induces the expression of the Rv0077c orthologue *bcg_0108c* in *M. bovis* bacillus Calmette-Guerin (15). Using X-ray crystallography and surface plasmon resonance techniques, the authors of this study found SMART-420 binds to Rv0078 to derepress binding from the Rv0077c promoter (14, 15). SMART-420 was identified in a search for compounds that boost the efficacy of the second-line tuberculosis drug ethionamide (ETH). ETH is a prodrug that is activated by the mono-oxygenase EthA, which transforms ETH into highly reactive intermediates. Activated ETH and NAD form a stable adduct that binds to and inhibits InhA, an essential enzyme needed for mycolic acid synthesis in mycobacteria (16, 17). While spontaneous inactivating mutations in *ethA* result in resistance to ETH, it was proposed that the induction of Rv0077c expression could bypass the need for EthA and transform ETH into its toxic form (15). Based on this study, we predicted that an Rv0078 mutant of *M. tuberculosis*, which expresses high levels of Rv0077c, should be hypersensitive to ETH compared to the parental strain H37Rv. However, we observed either little to no significant change in the 50% inhibitory concentration (IC₅₀) of ETH between the WT and ΔRv0078::hyg strains (Table 4) or in WT *M. tuberculosis* H37Rv treated with or without 100 μM iP (IC₅₀, 1.4). We also tested if the constitutive expression of Rv0077c changed the susceptibility of *M. tuberculosis* to other antibiotics, including two cell wall synthesis inhibitors. We observed no differences in the IC₅₀s of these antibiotics between the WT and ΔRv0078::hyg strains (Table 4).

We also tested if either the Rv0077c or Rv0078 mutant had growth defects *in vivo* compared to the WT H37Rv strain. We infected C57BL/6J mice by a low-dose aerosol route with the parental, mutant, and complemented mutant strains, as well as with the Rv0078 mutant transformed with the Rv0078_{W100R} allele. None of the strains revealed a difference in growth or survival compared to WT *M. tuberculosis* in mice, as determined by the recovery of CFU from the lungs and spleens (Fig. 5; see Fig. S3 in the supplemental material).

Expression of Rv0077c alters acid-fast staining of *M. tuberculosis*. To gain insight into the function of Rv0077c, we performed metabolomic analysis of strains expressing Rv0077c to potentially determine how its presence alters bacterial physiology. We prepared total cell lysates of WT and Rv0077c mutant strains treated with or without 100 μM iP for 24 h (see Materials and Methods). From a total of 337 detectable metabolites, we observed a significant change in 24 molecules after the addition of iP to WT *M. tuberculosis*. Seventeen metabolites showed a consistent difference between samples in which iP was added, and these changes disappeared in an Rv0077c-disrupted strain, suggesting the changes were specifically due to the presence of Rv0077c (Table S2, highlighted in yellow). We observed an increased abundance of several phospholipids and a decrease in a major precursor of peptidoglycan, *N*-acetylglucosamine-1-phosphate (GlcNAc1P). We therefore hy-

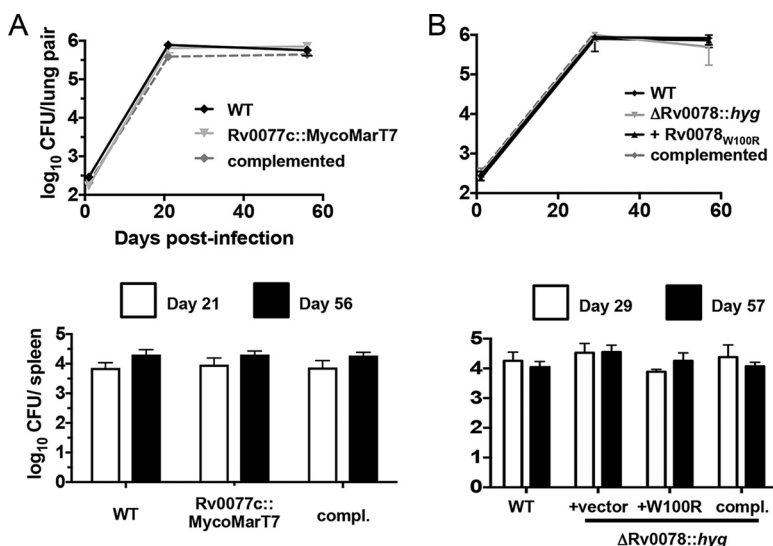


FIG 5 Loss of Rv0077c or Rv0078 does not attenuate bacterial survival in mice. (A) Bacterial CFU after infection of C57BL/6J mice with the WT, Rv0077c mutant, and complemented strains. (B) Bacterial CFU after infection of C57BL/6J mice with the WT, Rv0078 mutant, and complemented strains. For both panels, data in each are from a single experiment that is representative of two independent experiments. Error bars indicate the standard error of the mean.

pothesized that Rv0077c modified one or more components of the cell envelope. Microscopic examination of Ziehl-Neelsen (ZN)-stained WT *M. tuberculosis* treated with iP showed a loss of acid-fast staining (Fig. 6a versus b), and this phenotype depended on the presence of Rv0077c (Fig. 6c versus d). Complementation of the mutation with Rv0077c alone restored the iP-induced loss of acid-fast staining (Fig. 6e and f). Deletion of Rv0078 resulted in a constitutive loss of staining, irrespective of the presence of iP (Fig. 6g and h). Complementation of the Rv0078 deletion with the WT gene restored iP control of loss of acid-fast staining (Fig. 6i and j), but complementation with Rv0078_{W100R}, which could not fully derepress Rv0077c expression in the presence of iP (Fig. 2C), could not restore iP-induced loss of acid-fast staining (Fig. 6k and l). Mixing and simultaneous staining of the Rv0077c and Rv0078 mutants further showed the staining differences were not a result of a technical artifact (Fig. 6m). We also tested whether or not a carbolfuchsin (the primary stain in ZN staining) could interact at all with bacteria expressing Rv0077c and found that both the Rv0078 mutant and the parental strain stained equally well (Fig. 6n and o). This result suggested Rv0077c-expressing bacteria could bind to stain but not retain it after acid washing.

Acid-fast staining is primarily thought to be associated with mycolic acids; alterations in mycolic acid synthesis result in negative effects on cell growth *in vitro* and *in vivo* (18, 19). We used thin-layer and liquid or gas chromatography coupled to mass spectrometry to analyze the fatty acid, mycolic acid, and lipid contents of the WT and Rv0077c and Rv0078 mutant strains and observed no significant qualitative or quantitative differences between strains (see Fig. S4 and S5 and Table S3 in the supplemental material). In particular, the expression of Rv0077c did not conspicuously modify the chain length of mycolic acids, their cyclopropanation, or the relative abundance of keto- to α -mycolates and did not alter the wax ester and triglyceride contents of the strains that have previously been linked to acid-fast staining (19, 20).

DISCUSSION

Our studies are the first to demonstrate CKs induce robust and specific transcriptional and physiological changes in a bacterial species. *M. tuberculosis* treated with CK expressed high levels of Rv0077c, which altered its metabolome and staining properties. Despite these changes, we did not observe an effect on the susceptibility of these bacteria to antibiotics of different classes or on survival in mice. In addition we found

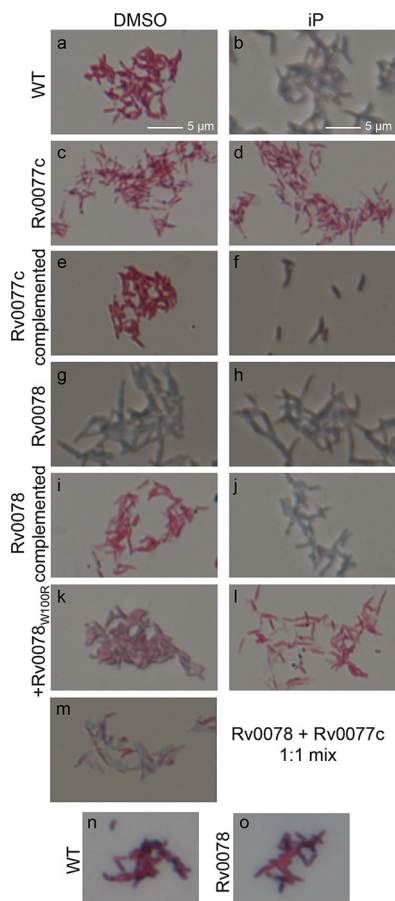


FIG 6 Induction of Rv0077c expression results in loss of acid-fast staining. *M. tuberculosis* strains were examined by Ziehl-Neelsen staining. The magnification is 63-fold. Scale bars are applicable to images in panels a to m. See text for details. “Rv0077c” indicates the Rv0077c::MycMarT7 strain and “Rv0078” indicates the Δ Rv0078::hyg strain.

the transcriptional regulator Rv0078 represses Rv0077c expression in the absence of CK, and we defined the operator to which Rv0078 binds. We determined that two dimers of Rv0078 bind to inverted repeats in the intergenic region between Rv0077c and Rv0078, which likely represses the expression of both genes.

In plants, CKs are sensed by membrane receptors related to the sensors of bacterial two-component systems (TCSs) (21–23). In these systems, CKs interact with membrane receptors via a CHASE (cylases/histidine kinases associated sensing extracellular) domain (24, 25). As in bacteria, the ligand-receptor interaction stimulates a phosphorylation that ultimately leads to the phosphorylation of a response regulator protein, which either represses or activates gene expression. *M. tuberculosis* has at least 12 known TCSs, and none has a predicted CHASE domain (L. Aravind, February 2012, and I. Jouline, August 2017, personal communications). Thus, it remains to be determined if a TCS sensor protein is involved in CK signal transduction in *M. tuberculosis*.

It also remains to be determined what the natural ligand is for Rv0078; while SMART-420 binds robustly to Rv0078 (14, 15), the cytokinin iP did not bind to this TetR-like regulator in our studies. This result may not be surprising when considering SMART-420 and cytokinins bear no resemblance to each other. Furthermore, we could not cocrystallize iP with Rv0078 (data not shown). We hypothesize that the interaction of CK with an unknown receptor or enzyme leads to the synthesis of a small molecule (e.g., a lipid) that binds to Rv0078, resulting in the derepression of Rv0077c. This possibility may be supported by our observation that there is an increase in several phospholipids in iP-treated *M. tuberculosis*. We are currently working to identify factors required for CK-mediated gene induction.

Rv0077c is predicted to have an α/β -hydrolase fold (26), which can have a variety of substrate types (27). Based on our metabolomic and microscopy studies, we predict Rv0077c targets one or more components of the cell envelope. The identification of the natural target of Rv0077c may help provide new insight into the elusive molecular basis of acid-fastness of this human-exclusive pathogen. While it is well known that perturbations in mycolic acid synthesis result in loss of acid-fast staining (18, 19), our results may indicate that acid-fast staining can be affected by other changes in cell envelope chemistry. Alternatively, Rv0077c may have a subtle chemical effect that is undetectable using the available techniques for quantifying mycolic acids. Importantly, although our results show dramatic changes in acid-fast staining *in vitro*, we do not know if cytokinin signaling results in these alterations *in vivo*. It is possible that the production of Rv0077c only affects a partial pool of substrates within a subset of bacteria, the effects of which might not result in a total loss of staining as we observed *in vitro*.

While we did not observe any differences in bacterial burdens in mice infected with strains that either were disrupted for or constitutively expressed Rv0077c, it is possible that Rv0077c function might only be needed during very late or specific stages of infection. This idea may be supported by a previous observation that the cytokinin synthase *log* gene in *Mycobacterium marinum* is specifically expressed in late granulomas of infected frogs (28). Furthermore, mice might not provide an optimal model to observe a role for this pathway in tuberculosis.

A previous report suggested the expression of Rv0077c increases the sensitivity of *M. tuberculosis* to the antibiotic ETH. ETH must be activated by a monooxygenase, EthA, in order for it to be toxic to *M. tuberculosis* (16, 17). We found the expression of Rv0077c did not confer increased susceptibility to ETH or any other antibiotic we tested, an observation consistent with the likelihood that Rv0077c is not a monooxygenase. It is possible that the effects of SMART-420 are growth condition dependent, that this molecule affects another pathway to increase the susceptibility of *M. tuberculosis* to ETH, or that another SMART-420-induced enzyme and Rv0077c synergize to activate ETH (A. Baulard, personal communication). Irrespective of these possibilities, it is unlikely that Rv0077c has a considerable role in the activation of ETH. While a previous report named Rv0077c and Rv0078 “EthA2” and “EthR2,” respectively, we propose to rename them “LoaA” and “LoaR” for “loss of acid-fast staining A and repressor,” respectively, due to the lack of association of these proteins with ETH susceptibility.

Finally, our studies have opened the door to the possibility that numerous commensal and pathogenic microbes (including fungi) use cytokinins for intra- or interspecies communication in complex systems such as the gut microbiome. The identification of one or more CK receptors and the signal transduction pathway that leads to the induction of Rv0077c expression will likely lay the foundation for understanding CK signaling in hundreds of bacterial species.

MATERIALS AND METHODS

Bacterial strains, plasmids, primers, chemicals, and culture conditions. The bacterial strains, plasmids, and primer sequences used in this study are listed in Table S1. All primers for cloning and sequencing were from Invitrogen, Inc. *M. tuberculosis* strains were grown in Middlebrook 7H9 broth (Difco) supplemented with 0.2% glycerol, 0.05% Tween 80, 0.5% fraction V of bovine serum albumin (BSA), 0.2% dextrose, and 0.085% sodium chloride (“7H9c”). *M. tuberculosis* cultures were grown without shaking in 25- or 75-cm² vented flasks (Corning) at 37°C. 7H11 agar (Difco) supplemented with 0.5% glycerol and BBL TM Middlebrook OADC enrichment (BD) was used for growth on solid medium (“7H11”). *M. tuberculosis* was transformed as described previously (29). *E. coli* strains used for cloning and expression were grown in LB-Miller broth (Difco) at 37°C with aeration on a shaker or on LB agar. *E. coli* strains were chemically transformed as previously described (30). The final concentrations of antibiotics used for *M. tuberculosis* growth were as follows: kanamycin, 50 μ g/ml; hygromycin, 50 μ g/ml; and streptomycin, 25 μ g/ml. The final concentrations for *E. coli* growth were as follows: hygromycin, 150 μ g/ml; kanamycin, 100 μ g/ml; and streptomycin, 50 μ g/ml. AMP, adenine, and iP were purchased from Sigma. iPR, 2MeSiP, and 2MeSiPR were synthesized as previously described (31). The purity of the synthesized cytokinin and derivatives was >98% for each, as determined by high-performance liquid chromatography and mass spectrometry.

The Rv0077c::MycMarT7 mutant was isolated from a library of ordered transposon insertion mutants as previously described (3, 32). The Δ Rv0078::hyg mutant was made by deletion-disruption mutagenesis

as described in detail elsewhere using pYUB854 (33, 34). All mutants were confirmed by PCR using primers that annealed to sequence beyond the region used for making allelic exchange plasmids.

Protein purification and immunoblotting. DNA sequence encompassing the full-length Rv0078 or Rv0077c gene was cloned into pET24b(+) vector using primers listed in Table S1. Recombinant proteins were produced in *E. coli* ER2566 and purified under native conditions for Rv0078 and denaturing conditions for Rv0077c according to the manufacturer's specifications (Qiagen). Polyclonal rabbit antibodies were raised by Covance (Denver, PA). For all immunoblots, cell lysates or purified proteins were separated by sodium dodecyl sulfate-polyacrylamide gel electrophoresis (SDS-PAGE), transferred to nitrocellulose, and incubated with rabbit polyclonal antibodies to the protein of interest at a 1:1,000 dilution in 3% bovine serum albumin in Tris-buffered saline-Tween (TBST: 25 mM Tris-HCl [pH 7.4], 125 mM NaCl, 0.05% Tween 20 [pH 7.4]). Equal loading was determined by stripping the nitrocellulose membranes with 0.2 N NaOH for 5 min, rinsing, blocking, and incubating the nitrocellulose with polyclonal rabbit antibodies to dihydrodipicolinate acyltransferase (DlaT) (35). Horseradish peroxidase-conjugated anti-rabbit antibody (GE-Amersham Biosciences, Inc.) was used for chemiluminescent detection (SuperSignal West Pico; Thermo Fisher Scientific).

For crystallography studies of Rv0078-His₆, bacteria were grown at 37°C to an optical density at 600 nm (OD₆₀₀) of 0.5 to 0.6 before being induced with 0.5 mM IPTG (isopropyl-β-D-thiogalactopyranoside) and incubated at 16°C overnight. After being harvested by centrifugation, cells were lysed by passing through a microfluidizer cell disrupter in a mixture of 10 mM potassium phosphate (pH 8.0), 10 mM imidazole, and 500 mM NaCl. The homogenate was clarified by spinning at 27,000 × *g*, and the supernatant was applied to a HiTrap-Ni column (GE Healthcare) preequilibrated with the lysis buffer. Histidine-tagged protein was eluted with a 10 to 300 mM imidazole gradient in 10 mM potassium phosphate (pH 8.0) containing 300 mM NaCl. The Rv0078 fractions were further purified by a Superdex 75 column (16 by 1,000 mm; GE Healthcare) preequilibrated with 20 mM potassium phosphate (pH 8.0) and 300 mM NaCl. The purified Rv0078 was concentrated to 40 mg/ml for the crystallization screen.

RNA-Seq and 5' RACE. Three biological replicate cultures of WT *M. tuberculosis* were grown to an OD₆₀₀ of ~1 and incubated in 100 μM iP or DMSO (control) for 5 h. Cells were harvested and RNA was purified as described previously (33). Briefly, an equal volume of 4 M guanidinium isothiocyanate, 0.5% sodium *N*-lauryl sarcosine, and 25 mM trisodium citrate solution was added to cultures to arrest transcription. RNA was isolated with Trizol reagent (Invitrogen) and further purified using RNeasy Miniprep kits and DNase I (Qiagen). Transcriptome profiling by RNA-Seq was performed, and the results were analyzed as follows. RNA from *M. tuberculosis* cultures was extracted for library construction. Libraries were constructed and bar-coded with the Epicentre ScriptSeq Complete Gold Low Input (Illumina, Inc.) and sequenced on an Illumina HiSeq 2000 sequencer using version 3 reagents. Unique sequence reads were mapped to the corresponding reference genome, and reads per kilobase per million (RPKM) values were calculated in CLC (version 7.0.4). Genes with significantly different RPKM values were identified using the Significant Analysis for Microarray (SAM) statistical analysis component of MeV (36).

5' RACE was performed as described by the manufacturer (Invitrogen). Briefly, 1 μg of RNA was used as the template for cDNA production using a reverse primer 150 to 300 bp downstream of annotated translational start sites. A 3' poly(C) tail was added to cDNA by recombinant Tdt. The cDNA was then amplified using a nested reverse primer and a primer that anneals to the poly(C) tail. Products were cloned and sequenced. Likely transcriptional start sites were selected based on the clones that had the most nucleotide sequence upstream of the start codon.

EMSA. A series of double-stranded DNA probes consisting of sequences in the intergenic region between Rv0077c and Rv0078 were generated by annealing two complementary oligonucleotides and 5'-end IRDye700-labeled 14-nucleotide oligomers (5'-dye-GTGCCCTGGTCTGG-3') (Integrated DNA Technologies, Inc.). Binding assays were performed by incubating 100 nM probes and various concentrations of Rv0078 at room temperature for 30 min in a mixture of 20 mM HEPES (pH 7.5), 3 mM dithiothreitol (DTT), 0.1 mM EDTA, 100 mM KCl, 5% glycerol, 5 mg/ml bovine serum albumin (BSA), 10 mM MgCl₂, and 0.25% Tween 20 and were subsequently resolved in 6% polyacrylamide gels in 0.5× Tris-borate-EDTA (TBE) buffer. Mobility shifts of protein-DNA complex were visualized in Li-Cor Odyssey imager.

Crystallization and structure determination. DNA-free Rv0078 crystals were obtained by screening at 20°C using the sitting-drop vapor diffusion method. The C2 space group crystals were grown in 0.1 M sodium cacodylate, pH 6.4, and 1.3 M lithium-sulfate. SeMet substituted Rv0078 crystals with C2 space group were grown in a mixture of 0.1 M sodium cacodylate (pH 6.6), 1.3 M lithium sulfate, 0.2 M magnesium sulfate, and 2% polyethylene glycol 400 (PEG 400). Diffraction data to a resolution of 1.85 Å were collected at the Lilly Research Laboratories Collaborative Access Team (LRL-CAT) beamline of Advanced Photon Source (APS), Argonne National Laboratory, and were processed with Mosflm software (37). The program Hybrid-Substructure-Search in the Phenix package was used to locate the Se sites, and the initial phasing was carried out using the program Autosol of Phenix. The 2.7-Å map phased by the SAD method allowed us to build the Rv0078 model unambiguously. The native Rv0078 structure was subsequently determined by the program PHASER using SeMet-substituted Rv0078 as the initial search model. To obtain the Rv0078-DNA crystals, purified Rv0078 was cocrystallized with a 23-mer DNA duplex (5'-TTTACAAGCAGACTGCCGGTAAC-3') at a molar ratio of 2:1 (protein dimer to DNA) in the presence of 150 mM MgCl₂. The DNA-bound Rv0078 crystals were grown in the buffer containing only 0.2 M magnesium formate. Diffraction data to 3.0 Å were collected at the Life Sciences Collaborative Access Team (LS-CAT) beamline of APS and were processed with Mosflm. The Rv0078 DNA structure was determined by PHASER using DNA-free structure as the search model. All the refinements were performed using Phenix-refine (38). The statistics are provided in Table 3.

Mass spectrometry of fatty acids copurified with Rv0078. Fatty acids were extracted from 5 mg Rv0078 that was purified from *E. coli* and analyzed as described previously (39). Separation and identification of the fatty acid (FA) methyl esters were performed on an HP5975 gas chromatograph-mass spectrometer (Hewlett-Packard) fitted with a 60-m by 250- μ m SP-2340 capillary column (Supelco) with helium as the carrier gas.

ITC. The isothermal calorimetry (ITC) experiment was performed in a Microcal PEAQ-ITC at 25°C. The stirring speed was 750 rpm, and the interval between each titration was 150 s. The concentration of Rv0078 in the reaction cell was 25 μ M, and the concentration of the titration DNA ligand was 500 μ M. The recorded thermal data were analyzed using Microcal PEAQ-ITC analysis software.

IC₅₀ determination. To determine the IC₅₀ of each antibiotic, *M. tuberculosis* strains were grown to an OD₅₈₀ of ~0.7 and diluted into fresh medium to an OD₅₈₀ of 0.02. Diluted cultures were transferred to a 96-well microtiter plate containing triplicate two-fold serial dilutions of antibiotic. Cell-wall-active antibiotics (vancomycin and meropenem) were supplemented at all concentrations with 5 μ g/ml potassium clavulanate to inhibit the intrinsic β -lactamase activity of *M. tuberculosis*. After 5 days of incubation at 37°C, growth in each well was measured by OD₅₈₀. IC₅₀ values were interpolated from a nonlinear least-squares fit of log₂-transformed OD₅₈₀ measurements. Data are representative of two independent experiments. Antibiotics were purchased from Sigma-Aldrich (clavulanate, ethionamide, meropenem, rifampin, and vancomycin) or Thermo-Fisher Scientific (ciprofloxacin, ethambutol, isoniazid, norfloxacin, and streptomycin).

Mouse infections. Mouse infections were performed essentially as described previously (3). Seven- to 9-week-old female C57BL6/J mice (The Jackson Laboratory) were infected by aerosol to deliver ~200 bacilli per mouse, using a Glas-Col inhalation exposure system (Terre Haute, IN). The strains used were the WT strain (MHD761 or MHD794), an Rv0077c mutant (MHD1086), an Rv0077c mutant complemented strain (MHD1077), an Rv0078 mutant (MHD1315), an Rv0078 mutant strain complemented with WT Rv0078 (MHD1318), and an Rv0078_{WT100R} mutant (MHD1316). This study was performed in strict accordance with the recommendations in the *Guide for the Care and Use of Laboratory Animals* of the National Institutes for Health. Mice were humanely euthanized according to an approved Institutional Animal Care and Use Committee protocol at New York University School of Medicine. Lungs and spleens were harvested and homogenized in phosphate-buffered saline (PBS)–0.05% Tween 80 at the indicated time points to determine bacterial CFU.

Metabolomic analysis of *M. tuberculosis* cell lysates. Four independent cultures of each analyzed strain were grown in 7H9 to an OD₅₈₀ of ~0.7 and treated with iP in DMSO at a final concentration of 100 μ M or an equal volume of DMSO for 24 h. Bacteria were harvested the next day at an OD₅₈₀ of ~1. Sixty-five OD equivalents per replicate were processed by chloroform-methanol extraction (8, 40). Metabolomic profiling was performed by Metabolon, Inc.

Staining and microscopy. *M. tuberculosis* strains were grown to mid-logarithmic phase (OD₅₈₀ of ~0.5 to 0.7). Five microliters of culture was spotted onto glass slides and heat fixed over a flame or on a heat block (2 min, 95°C). Staining was performed according to the method of Ziehl-Neelsen as per the manufacturer's instructions (BD Stain Kit ZN). Images were acquired on a Zeiss Axio Observer with a Plan-Apochromat 63 \times /1.4 oil lens. Images were taken with an Axiocam503 camera at the New York University Langone Medical Center (NYULMC) Microscopy Laboratory.

Analysis of total lipids, mycolic acids, and shorter-chain fatty acids. For lipid analysis, 400-ml cultures were grown up to an OD₅₈₀ of ~0.7 and treated with iP in DMSO at a final concentration of 100 μ M or an equal volume of DMSO only for 24 h. Four hundred milliliters of Rv0077c and Rv0078 cultures was treated with DMSO only. Cells were washed three times in Dulbecco's phosphate-buffered saline (DPBS) and heated at 100°C for 45 min for sterilization before freezing at –20°C. Extraction of total lipids from bacterial cells and preparation of fatty acid and mycolic acid methyl esters from extractable lipids and delipidated cells followed earlier procedures (41). Total lipids and fatty acid/mycolic acid methyl esters were analyzed by one- and two-dimensional thin-layer chromatography (TLC) in a variety of solvent systems on aluminum-backed silica gel 60-precoated plates F₂₅₄ (E. Merck). TLC plates were revealed by spraying with cupric sulfate (10% in an 8% phosphoric acid solution) and heating. Alternatively, total lipids were run in both positive and negative mode, with the released fatty acids/mycolic acids run in negative mode only, on a high-resolution Agilent 6220 time of flight (TOF) mass spectrometer interfaced to a liquid chromatograph as described previously (42, 43). Data files were analyzed with Agilent's Mass Hunter workstation software, and most compounds were identified using a database of *M. tuberculosis* lipids developed in house (42). Fatty acid methyl esters from extractable lipids were treated with 3 M HCl in CH₃OH (Supelco) overnight at 80°C, dried, and dissolved in *n*-hexane(s) prior to GC-MS analysis. GC-MS analyses of fatty acid methyl esters were carried out using a Trace 1310 gas chromatograph (Thermo Fisher) equipped with a TSQ 8000 Evo triple quadrupole in the electron impact mode and scanning from *m/z* 70 to *m/z* 1,000 over 0.8 s. Helium was used as the carrier gas with a flow rate of 1 ml per min. The samples were run on a ZB-5HT column (15 m by 0.25-mm inside diameter [i.d.] (Zebron). The injector (splitless mode) was set for 300°C (350°C for mycolic acid methyl esters). The oven temperature was held at 60°C for 2 min, programmed at 20°C per min to 375°C, followed by a 10-min hold. The data analyses were carried out on a Chromeleon data station.

SUPPLEMENTAL MATERIAL

Supplemental material for this article may be found at <https://doi.org/10.1128/mBio.00989-18>.

FIG S1, PDF file, 0.1 MB.

FIG S2, PDF file, 1 MB.

FIG S3, PDF file, 0.2 MB.

FIG S4, PDF file, 1.6 MB.

FIG S5, PDF file, 0.5 MB.

TABLE S1, XLSX file, 0.9 MB.

TABLE S2, XLSX file, 0.3 MB.

TABLE S3, DOCX file, 0.1 MB.

ACKNOWLEDGMENTS

We thank A. Darwin and V. Torres for critical review of a draft version of the manuscript. We thank S. Zhang for assistance in preparing reagents and E. Ballister for assistance with microscopy. We also thank A. Liang and Y. Deng of the Microscopy Laboratory at New York University Langone Medical Center for assistance with microscopy and imaging.

This work was supported by NIH grant R01 HL092774 awarded to K.H.D. K.H.D. holds an Investigators in the Pathogenesis of Infectious Disease Award from the Burroughs Wellcome Fund. M.I.S. and S.H.B. were supported by the Jan T. Vilcek Endowed Fellowship fund. S.H.B. is also supported by NIH grant T32 AT007180. H.C.H. and H.L. were supported by R01 AI070285. M. Strnad was supported by LO1204 from the National Program of Sustainability I and by 17-14007S from the Czech Grant Agency. Diffraction data for this study were collected at the Lilly Research Laboratories Collaborative Access Team (LRL-CAT) beamline and the Life Sciences Collaborative Access Team (LS-CAT) beamline at the Advanced Photon Source (APS), Argonne National Laboratory. The APS was supported by the U.S. Department of Energy, Office of Science, Office of Basic Energy Sciences, under contract DE-AC02-06CH11357. Use of the LRL-CAT beamline at sector 31 of the APS was provided by Eli Lilly Co., which operates the facility.

M.I.S. and K.H.D. performed *in vitro* and *in vivo* *M. tuberculosis* work. H.C.H. and H.L. determined the structure of Rv0078 and performed the mutagenesis and EMSAs. M.B.J. performed the RNA-Seq analysis. S.H.B. and A.T.J. performed antibiotic susceptibility assays. V.J., M.R.M., and M.J. performed the lipid analysis. C.X. performed mass spectrometry of fatty acids extracted from purified Rv0078 protein. M.S. synthesized cytokinins and their precursors. M.I.S., H.C.H., H.L., and K.H.D. wrote the manuscript.

REFERENCES

1. WHO. 2017. Tuberculosis. World Health Organization, Geneva, Switzerland. <http://www.who.int/mediacentre/factsheets/fs104/en/>.
2. Cerda-Maira FA, Pearce MJ, Fuortes M, Bishai WR, Hubbard SR, Darwin KH. 2010. Molecular analysis of the prokaryotic ubiquitin-like protein (Pup) conjugation pathway in *Mycobacterium tuberculosis*. *Mol Microbiol* 77:1123–1135. <https://doi.org/10.1111/j.1365-2958.2010.07276.x>.
3. Darwin KH, Ehrt S, Gutierrez-Ramos JC, Weich N, Nathan CF. 2003. The proteasome of *Mycobacterium tuberculosis* is required for resistance to nitric oxide. *Science* 302:1963–1966. <https://doi.org/10.1126/science.1091176>.
4. Gandotra S, Lebron MB, Ehrt S. 2010. The *Mycobacterium tuberculosis* proteasome active site threonine is essential for persistence yet dispensable for replication and resistance to nitric oxide. *PLoS Pathog* 6:e1001040. <https://doi.org/10.1371/journal.ppat.1001040>.
5. Gandotra S, Schnappinger D, Monteleone M, Hillen W, Ehrt S. 2007. In vivo gene silencing identifies the *Mycobacterium tuberculosis* proteasome as essential for the bacteria to persist in mice. *Nat Med* 13: 1515–1520. <https://doi.org/10.1038/nm1683>.
6. Lamichhane G, Raghunand TR, Morrison NE, Woolwine SC, Tyagi S, Kandavelou K, Bishai WR. 2006. Deletion of a *Mycobacterium tuberculosis* proteasomal ATPase homologue gene produces a slow-growing strain that persists in host tissues. *J Infect Dis* 194:1233–1240. <https://doi.org/10.1086/508288>.
7. Lin G, Li D, de Carvalho LP, Deng H, Tao H, Vogt G, Wu K, Schneider J, Chidawanyika T, Warren JD, Li H, Nathan C. 2009. Inhibitors selective for mycobacterial versus human proteasomes. *Nature* 461:621–626. <https://doi.org/10.1038/nature08357>.
8. Samanovic MI, Tu S, Novák O, Iyer LM, McAllister FE, Aravind L, Gygi SP, Hubbard SR, Strnad M, Darwin KH. 2015. Proteasomal control of cytokinin synthesis protects *Mycobacterium tuberculosis* against nitric oxide. *Mol Cell* 57:984–994. <https://doi.org/10.1016/j.molcel.2015.01.024>.
9. Sakakibara H. 2006. Cytokinins: activity, biosynthesis, and translocation. *Annu Rev Plant Biol* 57:431–449. <https://doi.org/10.1146/annurev.arplant.57.032905.105231>.
10. Frébort I, Kowalska M, Hluska T, Frébortová J, Galuszka P. 2011. Evolution of cytokinin biosynthesis and degradation. *J Exp Bot* 62:2431–2452. <https://doi.org/10.1093/jxb/err004>.
11. Lechat P, Hummel L, Rousseau S, Moszer I. 2008. Genolist: an integrated environment for comparative analysis of microbial genomes. *Nucleic Acids Res* 36:D469–D474. <https://doi.org/10.1093/nar/gkm1042>.
12. Brosch R, Gordon SV, Marmiesse M, Brodin P, Buchrieser C, Eiglmeier K, Garnier T, Gutierrez C, Hewinson G, Kremer K, Parsons LM, Pym AS, Samper S, van Soolingen D, Cole ST. 2002. A new evolutionary scenario for the *Mycobacterium tuberculosis* complex. *Proc Natl Acad Sci U S A* 99:3684–3689. <https://doi.org/10.1073/pnas.052548299>.
13. Orth P, Schnappinger D, Hillen W, Saenger W, Hinrichs W. 2000. Structural basis of gene regulation by the tetracycline inducible Tet repressor-operator system. *Nat Struct Biol* 7:215–219. <https://doi.org/10.1038/73324>.
14. Wohlkönig A, Remaut H, Moune M, Tanina A, Meyer F, Desroses M, Steyaert J, Willand N, Baulard AR, Wintjens R. 2017. Structural analysis of the interaction between spiroisoxazoline SMARt-420 and the *Mycobac-*

- terium tuberculosis repressor EthR2. *Biochem Biophys Res Commun* 487:403–408. <https://doi.org/10.1016/j.bbrc.2017.04.074>.
15. Blondiaux N, Moune M, Desroses M, Frita R, Flipo M, Mathys V, Soetaert K, Kiass M, Delorme V, Djaout K, Trebosc V, Kemmer C, Wintjens R, Wohlkönig A, Antoine R, Huot L, Hot D, Coscolla M, Feldmann J, Gagneux S, Loch C, Brodin P, Gitzinger M, Déprez B, Willand N, Baulard AR. 2017. Reversion of antibiotic resistance in *Mycobacterium tuberculosis* by spiroisoxazoline SMARt-420. *Science* 355:1206–1211. <https://doi.org/10.1126/science.aag1006>.
 16. DeBarber AE, Mdluli K, Bosman M, Bekker LG, Barry CE, III. 2000. Ethionamide activation and sensitivity in multidrug-resistant *Mycobacterium tuberculosis*. *Proc Natl Acad Sci U S A* 97:9677–9682. <https://doi.org/10.1073/pnas.97.17.9677>.
 17. Vannelli TA, Dykman A, Ortiz de Montellano PR. 2002. The antituberculosis drug ethionamide is activated by a flavoprotein monooxygenase. *J Biol Chem* 277:12824–12829. <https://doi.org/10.1074/jbc.M110751200>.
 18. Barkan D, Liu Z, Sacchetti JC, Glickman MS. 2009. Mycolic acid cyclopropanation is essential for viability, drug resistance, and cell wall integrity of *Mycobacterium tuberculosis*. *Chem Biol* 16:499–509. <https://doi.org/10.1016/j.chembiol.2009.04.001>.
 19. Bhatt A, Fujiwara N, Bhatt K, Gurcha SS, Kremer L, Chen B, Chan J, Porcelli SA, Kobayashi K, Besra GS, Jacobs WR, Jr. 2007. Deletion of *kasB* in *Mycobacterium tuberculosis* causes loss of acid-fastness and subclinical latent tuberculosis in immunocompetent mice. *Proc Natl Acad Sci U S A* 104:5157–5162. <https://doi.org/10.1073/pnas.0608654104>.
 20. Deb C, Lee CM, Dubej VS, Daniel J, Abomoelak B, Sirakova TD, Pawar S, Rogers L, Kolattukudy PE. 2009. A novel in vitro multiple-stress dormancy model for *Mycobacterium tuberculosis* generates a lipid-loaded, drug-tolerant, dormant pathogen. *PLoS One* 4:e6077. <https://doi.org/10.1371/journal.pone.0006077>.
 21. To JP, Kieber JJ. 2008. Cytokinin signaling: two-components and more. *Trends Plant Sci* 13:85–92. <https://doi.org/10.1016/j.tplants.2007.11.005>.
 22. Inoue T, Higuchi M, Hashimoto Y, Seki M, Kobayashi M, Kato T, Tabata S, Shinozaki K, Kakimoto T. 2001. Identification of CRE1 as a cytokinin receptor from *Arabidopsis*. *Nature* 409:1060–1063. <https://doi.org/10.1038/35059117>.
 23. Steklov MY, Lomin SN, Osolodkin DI, Romanov GA. 2013. Structural basis for cytokinin receptor signaling: an evolutionary approach. *Plant Cell Rep* 32:781–793. <https://doi.org/10.1007/s00299-013-1408-3>.
 24. Mougel C, Zhulin IB. 2001. CHASE: an extracellular sensing domain common to transmembrane receptors from prokaryotes, lower eukaryotes and plants. *Trends Biochem Sci* 26:582–584. [https://doi.org/10.1016/S0968-0004\(01\)01969-7](https://doi.org/10.1016/S0968-0004(01)01969-7).
 25. Anantharaman V, Aravind L. 2001. The CHASE domain: a predicted ligand-binding module in plant cytokinin receptors and other eukaryotic and bacterial receptors. *Trends Biochem Sci* 26:579–582. [https://doi.org/10.1016/S0968-0004\(01\)01968-5](https://doi.org/10.1016/S0968-0004(01)01968-5).
 26. Söding J, Biegert A, Lupas AN. 2005. The HHpred interactive server for protein homology detection and structure prediction. *Nucleic Acids Res* 33:W244–W248. <https://doi.org/10.1093/nar/gki408>.
 27. Nardini M, Dijkstra BW. 1999. Alpha/beta hydrolase fold enzymes: the family keeps growing. *Curr Opin Struct Biol* 9:732–737. [https://doi.org/10.1016/S0959-440X\(99\)00037-8](https://doi.org/10.1016/S0959-440X(99)00037-8).
 28. Ramakrishnan L, Federspiel NA, Falkow S. 2000. Granuloma-specific expression of *Mycobacterium tuberculosis* virulence proteins from the glycine-rich PE-PGRS family. *Science* 288:1436–1439. <https://doi.org/10.1126/science.288.5470.1436>.
 29. Hatfull GF, Jacobs WRJ. 2000. *Molecular genetics of mycobacteria*. ASM Press, Washington, DC.
 30. Sambrook J, Maniatis T, Fritsch E. 1989. *Molecular cloning: a laboratory manual*, 2nd ed. Cold Spring Harbor Laboratory Press, Cold Spring Harbor, NY.
 31. Sugiyama T, Hashizume T. 1978. Ribosylation of 6-chloropurine and its 2-methylthio derivative by a fusion procedure using iodine. *Agric Biol Chem* 42:1791–1792.
 32. Festa RA, Pearce MJ, Darwin KH. 2007. Characterization of the protease accessory factor (*paF*) operon in *Mycobacterium tuberculosis*. *J Bacteriol* 189:3044–3050. <https://doi.org/10.1128/JB.01597-06>.
 33. Festa RA, Jones MB, Butler-Wu S, Sinsimer D, Gerads R, Bishai WR, Peterson SN, Darwin KH. 2011. A novel copper-responsive regulon in *Mycobacterium tuberculosis*. *Mol Microbiol* 79:133–148. <https://doi.org/10.1111/j.1365-2958.2010.07431.x>.
 34. Bardarov S, Bardarov S, Jr, Pavelka MS, Jr, Sambandamurthy V, Larsen M, Tufariello J, Chan J, Hatfull G, Jacobs WR, Jr. 2002. Specialized transduction: an efficient method for generating marked and unmarked targeted gene disruptions in *Mycobacterium tuberculosis*, *M. bovis* BCG and *M. smegmatis*. *Microbiology* 148:3007–3017. <https://doi.org/10.1099/00221287-148-10-3007>.
 35. Tian J, Bryk R, Shi S, Erdjument-Bromage H, Tempst P, Nathan C. 2005. *Mycobacterium tuberculosis* appears to lack alpha-ketoglutarate dehydrogenase and encodes pyruvate dehydrogenase in widely separated genes. *Mol Microbiol* 57:859–868. <https://doi.org/10.1111/j.1365-2958.2005.04741.x>.
 36. Saeed AI, Sharov V, White J, Li J, Liang W, Bhagabati N, Braisted J, Klapa M, Courier T, Thiagarajan M, Sturn A, Snuffin M, Rezantsev A, Popov D, Ryltsov A, Kostukovich E, Borisovsky I, Liu Z, Vinsavich A, Trush V, Quackenbush J. 2003. TM4: a free, open-source system for microarray data management and analysis. *Biotechniques* 34:374–378.
 37. Winn MD, Ballard CC, Cowtan KD, Dodson EJ, Emsley P, Evans PR, Keegan RM, Krissinel EB, Leslie AG, McCoy A, McNicholas SJ, Murshudov GN, Pannu NS, Potterton EA, Powell HR, Read RJ, Vagin A, Wilson KS. 2011. Overview of the CCP4 suite and current developments. *Acta Crystallogr D Biol Crystallogr* 67:235–242. <https://doi.org/10.1107/S0907444910045749>.
 38. Adams PD, Afonine PV, Bunkóczi G, Chen VB, Davis IW, Echols N, Headd JJ, Hung LW, Kapral GJ, Grosse-Kunstleve RW, McCoy AJ, Moriarty NW, Oeffner R, Read RJ, Richardson DC, Richardson JS, Terwilliger TC, Zwart PH. 2010. PHENIX: a comprehensive Python-based system for macromolecular structure solution. *Acta Crystallogr D Biol Crystallogr* 66:213–221. <https://doi.org/10.1107/S0907444909052925>.
 39. Fan J, Yan C, Xu C. 2013. Phospholipid:diacylglycerol acyltransferase-mediated triacylglycerol biosynthesis is crucial for protection against fatty acid-induced cell death in growing tissues of *Arabidopsis*. *Plant J* 76:930–942. <https://doi.org/10.1111/tpj.12343>.
 40. Layre E, Sweet L, Hong S, Madigan CA, Desjardins D, Young DC, Cheng TY, Annand JW, Kim K, Shamputa IC, McConnell MJ, Debono CA, Behar SM, Minnaard AJ, Murray M, Barry CE, III, Matsunaga I, Moody DB. 2011. A comparative lipidomics platform for chemotaxonomic analysis of *Mycobacterium tuberculosis*. *Chem Biol* 18:1537–1549. <https://doi.org/10.1016/j.chembiol.2011.10.013>.
 41. Stadthagen G, Korduláková J, Griffin R, Constant P, Bottová I, Barilone N, Gicquel B, Daffé M, Jackson M. 2005. p-Hydroxybenzoic acid synthesis in *Mycobacterium tuberculosis*. *J Biol Chem* 280:40699–40706. <https://doi.org/10.1074/jbc.M508332200>.
 42. Sartain MJ, Dick DL, Rithner CD, Crick DC, Belisle JT. 2011. Lipidomic analyses of *Mycobacterium tuberculosis* based on accurate mass measurements and the novel “Mtb LipidDB”. *J Lipid Res* 52:861–872. <https://doi.org/10.1194/jlr.M010363>.
 43. Bhamidi S, Shi L, Chatterjee D, Belisle JT, Crick DC, McNeil MR. 2012. A bioanalytical method to determine the cell wall composition of *Mycobacterium tuberculosis* grown in vivo. *Anal Biochem* 421:240–249. <https://doi.org/10.1016/j.ab.2011.10.046>.
 44. Shi X, Festa RA, Iøerger TR, Butler-Wu S, Sacchetti JC, Darwin KH, Samanovic MI. 2014. The copper-responsive RicR regulon contributes to *Mycobacterium tuberculosis* virulence. *mBio* 5:e00876-13. <https://doi.org/10.1128/mBio.00876-13>.
 45. Chong YH, Jung JM, Choi W, Park CW, Choi KS, Suh YH. 1994. Bacterial expression, purification of full length and carboxyl terminal fragment of Alzheimer amyloid precursor protein and their proteolytic processing by thrombin. *Life Sci* 54:1259–1268. [https://doi.org/10.1016/0024-3205\(94\)00853-1](https://doi.org/10.1016/0024-3205(94)00853-1).
 46. Stover CK, de la Cruz VF, Fuerst TR, Burlein JE, Benson LA, Bennett LT, Bansal GP, Young JF, Lee MH, Hatfull GF, Snapper SB, Barletta RG, Jacobs WR, Jr, Bloom BR. 1991. New use of BCG for recombinant vaccines. *Nature* 351:456–460. <https://doi.org/10.1038/351456a0>.